Available online at www.sciencedirect.com
ScienceDirect
Thermochimica Acta 457 (2007) 92–102
thermochimica acta
www.elsevier.com/locate/tca

Thermal degradation of commercially available organoclays studied by TGA–FTIR

José M. Cervantes-Uc [a,*], Juan V. Cauich-Rodríguez [a], Humberto Vázquez-Torres [b], Luis F. Garfias-Mesías [c], Donald R. Paul [d]

[a] *Centro de Investigación Científica de Yucatán, A.C., Calle 43 No. 130, Col. Chuburná de Hidalgo, C.P. 97200, Mérida, Yucatán, Mexico*
[b] *Universidad Autónoma Metropolitana-Iztapalapa, Departamento de Física, San Rafael Atlixco No. 186, Col. Vicentina, C.P. 09340, México, D.F., Mexico*
[c] *RD&E, Corrosion Laboratory, S. C. Johnson & Son, Inc., 1525 Howe Street, M/S #051, Racine, WI 53403, USA*
[d] *Department of Chemical Engineering and Texas Materials Institute, University of Texas at Austin, TX 78712, USA*

Received 26 December 2006; received in revised form 9 February 2007; accepted 12 March 2007
Available online 15 March 2007

Abstract

Thermogravimetry coupled to Fourier transform infrared spectroscopy (TGA/FTIR) has been used to study the thermal decomposition products evolved during the degradation of several commercially available organoclays (Cloisites™ Na^+, 10A, 15A, 20A, 25A, 93A and 30B). It was found that the decomposition pattern of the organoclays was different for each sample: Cloisite™ 10A shows three well-defined degradation stages, Cloisite™ 30B only two stages and the Cloisite™ 93A only one weight loss; Cloisites™ 15A, 20A and 25A exhibited a more complex behavior showing one main stage and a shoulder. It was also observed that the onset of the decomposition was different for each type of organoclay, being Cloisite™ 10A the lowest (160 °C) and Cloisite™ 93A the highest (212 °C). FTIR analysis of the evolved products from their non-oxidative thermal degradation showed the release of water, aldehydes, carboxylic acids, aliphatic compounds and, in some cases, aromatic compounds and CO_2. It is suggested that the degradation of both tallow residue and unexchanged surfactant explain the presence of some products evolved during degradation of organoclays.

Keywords: Thermal degradation; Organoclay; Thermal decomposition; Cloisite™

1. Introduction

In recent years, polymer–clay nanocomposites have attracted a great deal of interest as they exhibit improvements in mechanical, thermal, barrier and flame-retardant properties compared to the neat or traditionally filled resins [1]. Clays used in the nanocomposites are those denominated as “organoclays”, cationic complexes in which the surface metal cations of natural clays have been exchanged with an organic cationic surfactant. The surfactant layer is organophilic allowing the inorganic clays to be dispersed in organic polymers [2]. Although the organoclays complexes, often alkyl ammonium compounds, have been recognized for a long time, the interest in studying these layered silicate materials as nanoscale reinforcing agents for polymeric materials has been developed recently [1].

Nanocomposites can be prepared by solvent casting, *in situ* polymerization and melt compounding, being the latter an attractive technique for manufacturing nanocomposites as it is suitable for most thermoplastics. Thus, for polymers that require high melt processing temperatures, the thermal stability of the organic component of the modified clay becomes a significant factor for a variety of reasons that are discussed below [3]. Thermogravimetric analysis has showed that the organic component of organoclays begins to breakdown at temperatures ca. 180 °C under non-oxidative environments, and significant degradation occurs just above this temperature [3,4]. Unfortunately, these degradation temperatures may be exceeded during the melt processing of many polymers, for instance HDPE, PP, nylon, TPU, etc. As a consequence, the onset of the thermal decomposition of the organic modifier in the clay, not the polymer, must set the top limit temperature for polymer processing. Therefore, it is of prime importance to study the thermal stability of the organic modifier and its implications on the nanocomposite processing and properties [1].

* Corresponding author. Tel.: +52 999 9813966; fax: +52 999 9813900.
E-mail address: manceruc@cicy.mx (J.M. Cervantes-Uc).

0040-6031/$ – see front matter © 2007 Elsevier B.V. All rights reserved.
doi:10.1016/j.tca.2007.03.008

It is worthy to mention that the degradation of organoclays and their decomposition products are often overlooked, but must be taken into account for understanding how the partially degraded clay and the chemicals released might affect the final nanocomposite properties and long term performance. In this sense, it has been reported that the degradation clays may affect the thermodynamics of polymer melt intercalation due to chemical changes in surfactant structure and thus altering the physical and mechanical properties. Furthermore, decomposition of the surfactant may produce undesired side reactions with the polymeric matrix [3].

Several authors [5–7] have studied the degradation of alkyl ammonium organoclays by means of thermogravimetry (TGA), Fourier transform infrared spectroscopy (FTIR), gas chromatography (GC), mass spectrometry (MS), pyrolysis, and the combination of these techniques, among others. The presence of alkanes, alkenes, chloro-alkanes, amines, aldehydes, etc., has been detected as part of the organic species evolved. However, many of the chemical species suggested as degradation products, through Hoffman elimination and SN_2 nucleophilic substitution, were not clearly associated to the chemical composition of the alkyl ammonium organoclays. Furthermore, the mechanisms through which the compounds were formed have not been established.

The aim of this work was to investigate the thermal degradation of various commercially available organoclays using thermogravimetry coupled with Fourier transform infrared spectroscopy (TGA/FTIR), considering the effect of the chemical structure of the quaternary alkyl ammonium modifier. Therefore, a comparison between thermal degradation products from several Cloisites™ was made. It is expected that this information might be useful to explain the degradation mechanism observed in nanocomposites where the evolved products interact with the polymeric matrix.

2. Experimental

2.1. Materials

Natural montmorillonite (Cloisite™ Na^+) and several commercial organically modified montmorillonites (Cloisite™ 10A, Cloisite™ 15A, Cloisite™ 20A, Cloisite™ 25A, Cloisite™ 30B and Cloisite™ 93A) from Southern Clay Products, Inc. were used in this study as received. The chemical structures of surfactants are displayed in Fig. 1 and the organoclays characteristics are summarized in Table 1. In Fig. 1, N^+ denotes a quaternary ammonium salt; T and HT denote tallow and hydrogenated tallow, respectively, which consist of ∼65% C18; ∼30% C16; ∼5% C14 (data taken from the Technical Properties Bulletin from Southern Clay Products).

2.2. Characterization of nanoclays

2.2.1. Elemental analysis

In order to know the chemical composition of all the montmorillonites used in the present study, elemental analysis was performed by means of a Perkin Elmer 2400 series II CHNS/O elemental analyzer. In addition, microanalysis was conducted with a JEOL JSM-6360 LV scanning electron microscope coupled with EDX (Oxford Instruments, INCA Energy 200).

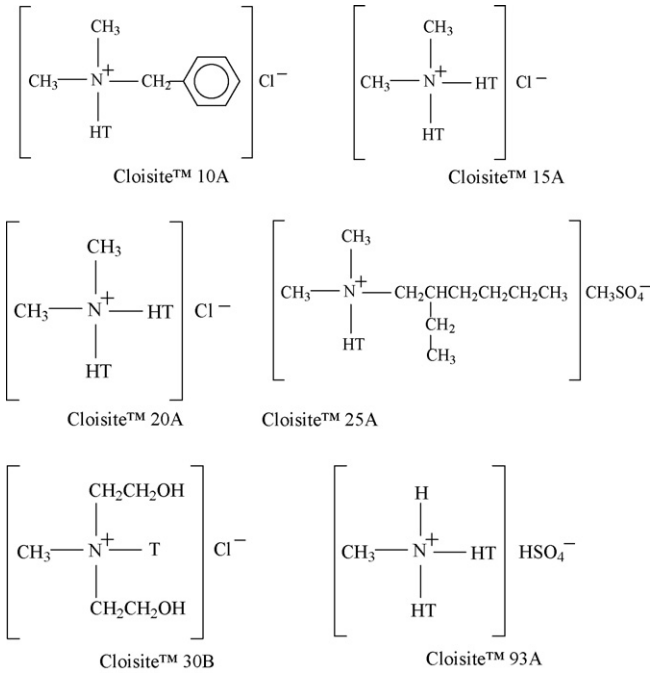

Fig. 1. Chemical structures of the organic modifiers (surfactants) used during organoclay formulation by Southern Clays Co.

2.2.2. Fourier transform infrared spectroscopy

Infrared spectra of the nanoclays were obtained from KBr pellets at room temperature using a Nicolet Magna Spectrometer with a resolution of 4 cm^{-1} averaging 50 scans in the 4000–650 cm^{-1} wavenumber range.

2.2.3. Thermogravimetric analysis

Thermogravimetric data were collected from 50 to 600 °C at 10 °C/min under dry nitrogen atmosphere by using a Perkin Elmer TGA-7. Sample masses ca. 10 mg were used.

Table 1
Characteristics of the organoclays used in this study

Sample code	Organic modifier (surfactant)	Anion
Cloisite™ Na^+	None	None
Cloisite™ 10A	Dimethyl, benzyl, hydrogenated tallow, quaternary ammonium	Chloride
Cloisite™ 15A	Dimethyl, dihydrogenated tallow, quaternary ammonium	Chloride
Cloisite™ 20A	Dimethyl, dihydrogenated tallow, quaternary ammonium	Chloride
Cloisite™ 25A	Dimethyl, dihydrogenated tallow, 2-ethylhexyl quaternary ammonium	Methyl sulfate
Cloisite™ 30B	Methyl, dihydrogenated tallow ammonium	Chloride
Cloisite™ 93A	Dimethyl, dihydrogenated tallow, ammonium	Bisulfate

2.3. Thermal degradation studies

Thermogravimetry coupled with Fourier transform infrared spectroscopy (TGA–FTIR) experiments were carried out with a TGA Pyris 1 at 10 °C/min. interfaced with a GX system FTIR spectrometer from Perkin-Elmer. Dry nitrogen gas carried the decomposition products through stainless steel line into the gas cell for IR detection. Both, the transfer line and the gas cell were kept at 250 °C to prevent gas condensation. IR spectra were recorded in the spectral range of 4000–650 cm^{-1} with a 4 cm^{-1} resolution and averaging 8 scans. Thirty-eight spectra were obtained for each sample. Samples masses ranging from 20 to 25 mg were used.

3. Results

3.1. Elemental analysis of non-degraded cloisites™

Table 2 summarizes the average chemical composition of each element (C, H and N) of the different Cloisites™. From EDX analysis, it was found the presence of metallic elements such as aluminum (8.5 wt%), iron (3.5 wt%) and magnesium (1.5 wt%), in addition to silicon (32 wt%). In natural montmorillonite sodium was detected at 2 wt% while for Cloisites™ 10A, 15A, 20A and 30B chlorine was detected in the range of 0.3–0.8 wt%. Oxygen was also present in the range of 31–45 wt%, whereas sulfur was detected for Cloisite™ 25A and 93A in the range of 0.14–0.19 wt%. The presence of chlorine and sulfur in these organoclays indicates that a part of surfactant has not been exchanged with sodium and remains as quaternary ammonium salt in the clay.

3.2. IR spectroscopy

FTIR spectra of sodium montmorillonite and those organically modified clays are shown in Fig. 2. As noted, all the spectra show bands at 3636 and 3395 cm^{-1} attributed to O–H stretching for the silicate and water, respectively, 1639 cm^{-1} (related to O–H bending), 1040 cm^{-1} (owing of stretching vibration of Si–O–Si from silicate) and 917 cm^{-1} (from Al–OH–Al deformation of aluminates) [4]. However, there are some bands in organoclays samples spectra which are not exhibited by the sodium clay; these bands were located at 2924, 2842 and 1475 cm^{-1} and were assigned to C–H vibrations of methylene groups (asymmetric stretching, symmetric stretching and bending, respectively) from chemical structure of the surfactant.

Table 2
Elemental chemical analysis of the Cloisites™

Sample code	Carbon (%)	Hydrogen (%)	Nitrogen (%)
Cloisite™ Na^+	0.70	0.9	0.1
Cloisite™ 10A	26.8	4.4	3.6
Cloisite™ 15A	31.0	5.6	4.2
Cloisite™ 20A	27.6	5.1	4.1
Cloisite™ 25A	23.8	4.3	3.6
Cloisite™ 30B	17.9	3.5	2.8
Cloisite™ 93A	25.6	4.7	3.5

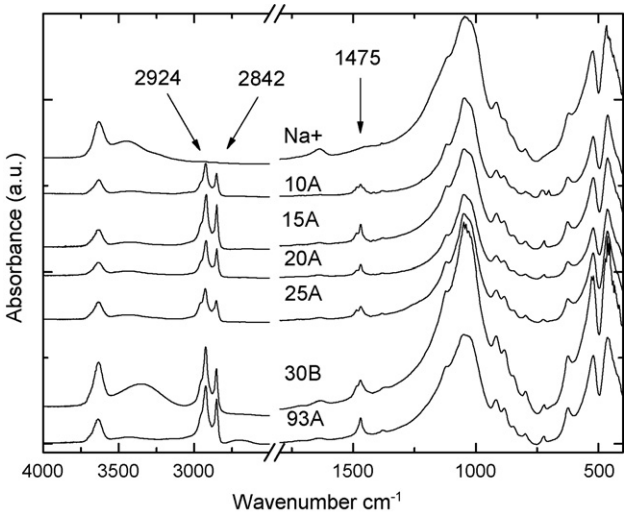

Fig. 2. FTIR spectra of various commercial clays.

3.3. Thermogravimetric analysis

Fig. 3 shows the TG weight loss curves and the corresponding derivate curves (DTG) of the nanoclays used in this study. As can be seen, the decomposition pattern of the organoclays was different for each sample; for instance, Cloisite™ 10A shows three well-defined degradation stages, Cloisite™ 30B only two stages and the Cloisite™ 93A only one weight loss. Cloisites™ 15A, 20A and 25A exhibited a more complex behavior showing one main stage and a shoulder.

The onset decomposition temperatures, the maximum mass loss rate temperatures for each degradation step and the residual masses of the Cloisites™ are shown in Table 3. In general, the residual mass values lie within the range reported by the manufacturer, except for Cloisite™ 93A, which presented a discrepancy of about 13%. Differences between values of residual mass obtained by TGA and those reported by manufacturer have been pointed out and it has been mentioned that this residue is composed of inorganic material like aluminosilicates and metallic oxides (Fe_2O_3, MgO, etc.) although the presence of carbonaceous organic residues is not discarded [6,8].

In general, it can be considered that the residual mass (inorganic material) does not play a key role in the thermal degradation pathway of organoclays; however, there are some reports [6,7] that indicate that the presence of oxygen and metal species in the montmorillonite structure (clay) may serve as catalyst to enable the oxidative cleavage of alkenes to produce aldehydes at elevated temperatures.

3.4. TGA–FTIR of degraded nanoclays

The obtained results from TGA–FTIR are presented as follows: a Gram–Schmidt plot, which shows information related with the total IR absorbance of the evolved components in whole spectral range; a three-dimensional spectra (as stack plot) of evolved gases and finally, the IR spectra obtained at the maximum evolution rate for each decomposition stage.

Table 3
The onset decomposition temperatures, the maximum mass loss rate temperatures and residual mass of the Cloisites™

Sample code	Onset decomposition temperature from TGA (°C)	Maximum mass loss rate temperature from DTGA(°C)	Residual mass (%)
Cloisite™ Na^+	–	–	95
Cloisite™ 10A	160	245, 310, 395	66
Cloisite™ 15A	192	331, 447	60
Cloisite™ 20A	198	336, 451	63
Cloisite™ 25A	192	330, 390	74
Cloisite™ 30B	174	298, 427	73
Cloisite™ 93A	212	347	76

3.4.1. *Cloisite™ Na^+*

As can be seen in Fig. 4a, there is no clear temperature range in which the evolved gases reach their maximum intensity but only a monotonic increment of the absorbance can be appreciated in the Gram–Schmidt graph. Also, FTIR spectra of the evolved gases (see Fig. 4b), obtained during the thermal degradation of pristine sodium montmorillonite (Cloisite™ Na^+), did not show any important band, except for signals attributed to moisture. Therefore, spectra at the maximum evolution rate for each decomposition step were not displayed. Water can be in the form of free water (generally released below 100 °C), bound water (below 300 °C) and structural water (near 600 °C). In this study, a small signal was detected below 300 °C and therefore attributed to a very small amount of bound water.

3.4.2. *Cloisite™ 10A*

The Gram–Schmidt plot for Cloisite™ 10A (Fig. 5a) exhibited a more complex behavior than those exhibited by other organoclays, i.e. the graph showed several evolved products regions located at 250, 315, 399 and 443 °C. Nevertheless, Fig. 5c does not show spectra obtained at 315 and 399 °C because these were very similar to that obtained at 443 °C, and in their

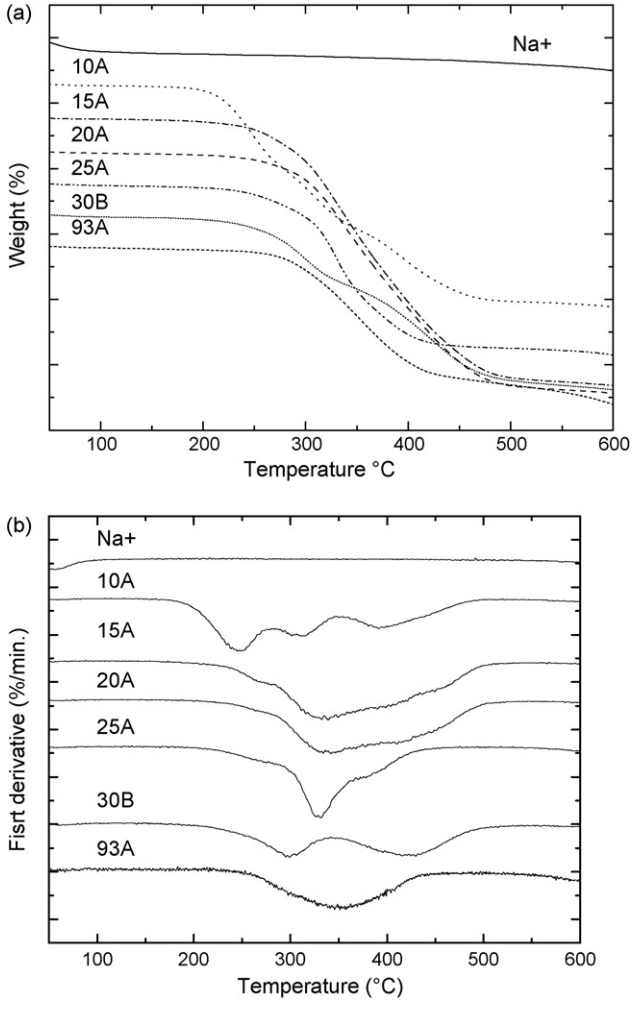

Fig. 3. Thermogravimetric analysis (a) and DTGA curves (b) of several commercial clays.

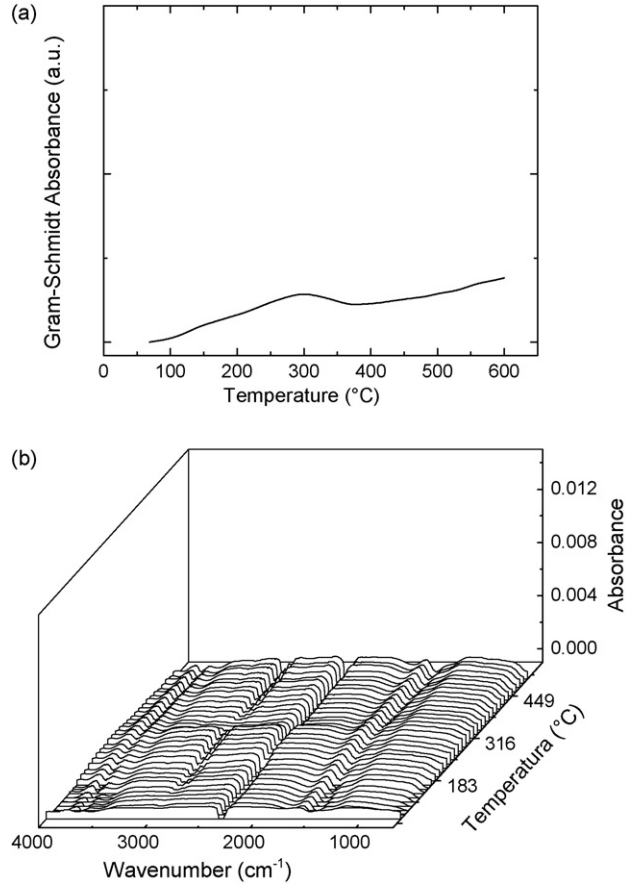

Fig. 4. Gram–Schmidt plot (a) and 3D-FTIR spectra of evolved gases (b) for sodium Cloisite™.

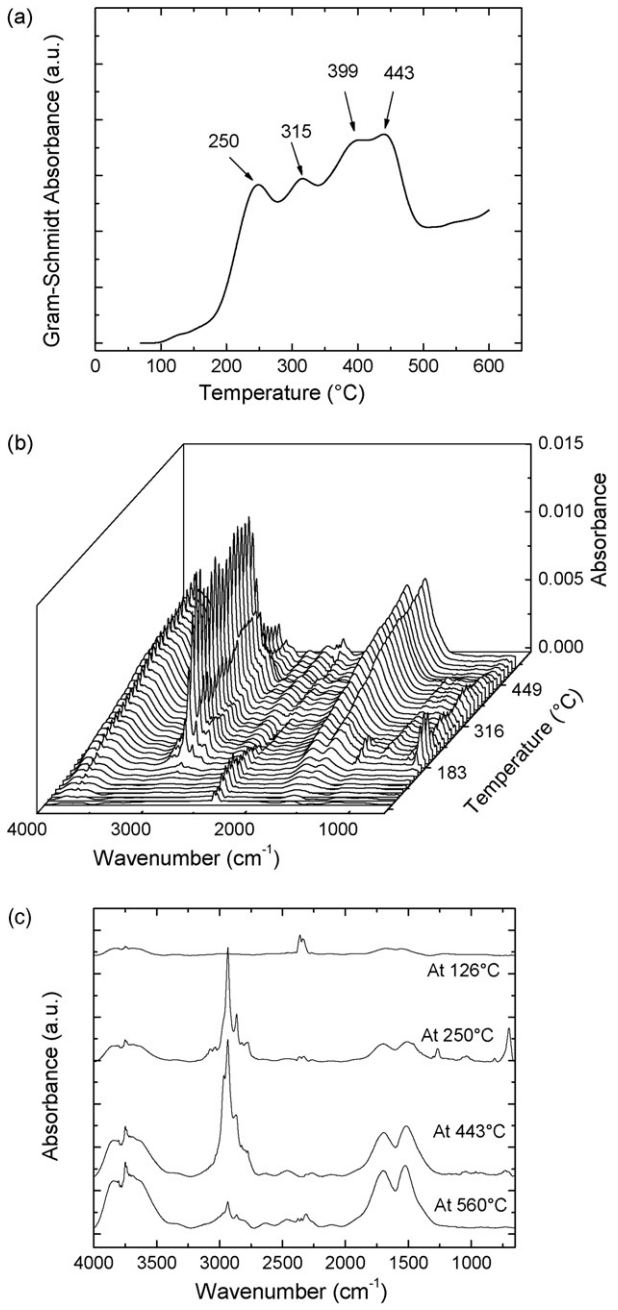

Fig. 5. Gram–Schmidt plot (a); 3D-FTIR spectra of evolved gases (b); and IR spectra obtained at several temperatures (c) for Cloisite^{TM} 10A.

place, the obtained spectra at 126 and 560 °C are displayed since they exhibited interesting results. The spectrum at 126 °C exhibited bands associated to O–H stretching (4000–3300 cm^{-1}) and bands attributed to CO_2 (2360 and 2340 cm^{-1}). At the temperature of 250 °C, which corresponded to the first evolved gases, the spectrum showed an increase in intensity of the signals associated with OH groups as well as a decrease in those bands related with CO_2. The appearance of bands attributed to C–H stretching from methyl and methylene groups, and bands at 1704 and 1508 cm^{-1} (related with O–H bending) were also noted. Furthermore, bands related with aromatic structures, were also detected at this stage. The obtained spectrum at 443 °C was similar to that obtained in the previous stage but the peaks assigned to aromatic compounds have disappeared and those located at ca. 3750, 1704 and 1508 cm^{-1} have increased in intensity. Finally, the spectrum obtained at 560 °C was very similar to that obtained in the previous stage, although the bands associated to aliphatic compounds vanished almost totally.

3.4.3. Cloisite^{TM} 15A

Fig. 6 shows the obtained results in the thermal degradation of the Cloisite^{TM} 15A. As noted in Fig. 6a, there were

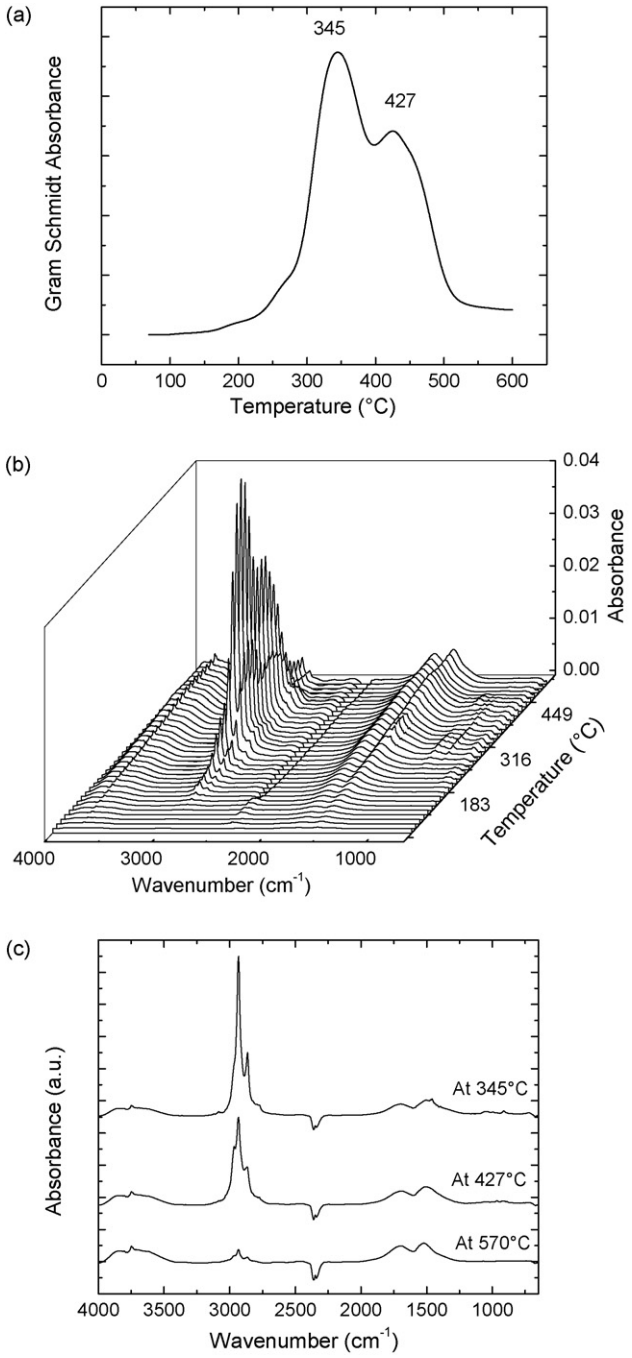

Fig. 6. Gram–Schmidt plot (a); 3D-FTIR spectra of evolved gases (b); and IR spectra obtained at several temperatures (c) for Cloisite^{TM} 15A.

two main gas discharges situated at 345 and 427 °C although by TGA only one complex decomposition temperature peaking at 335 °C was observed. FTIR spectra for both stages were very similar among them (see Fig. 6c) as they showed bands related with O–H stretching, C–H stretching of aliphatic compounds and two broad bands centered at 1700 and 1488 cm^{-1}. Fig. 6c also shows the spectrum obtained at 570 °C, in which the bands related to OH groups as well as those situated at 1700 and 1488 cm^{-1} remained but with lower intensity, whereas the bands corresponding to C–H stretching practically disappeared.

3.4.4. Cloisite™ 20A

Fig. 7a shows the Gram–Schmidt diagram of evolved products from Cloisite™ 20A. As can be seen, this sample exhibited only two main evolved gases regions at 332 and 414 °C, even though Fig. 7c also shows the spectra obtained at 241 and 514 °C.

Spectra of the evolved products at 332 and 414 °C were similar (see Fig. 7c) as they presented bands associated to compounds containing OH groups, bands attributed to C–H stretching of aliphatic compounds and two strong signals at 1720 and 1524 cm^{-1}. The only difference among them (spectra at 332 and 414 °C) was the intensity of the signals. The collected spectra at 241 and 514 °C which do not correspond to any maximum of evolved gases are included only for comparison. Indeed, these spectra were similar among them and to the spectra obtained at 332 and 414 °C, except for the bands related to C–H stretching of methyl and methylene groups that resulted in lower intensity.

3.4.5. Cloisite™ 25A

Thermal degradation behavior of the Cloisite™ 25A is shown in Fig. 8. As noted, this sample shows two main regions of gas emissions (see Fig. 8a). These emissions, located at 329 and 423 °C, gave similar spectra (see Fig. 8c) showing bands associated to OH groups; bands attributed to aliphatic compounds; bands centered at 1704 and 1524 cm^{-1} and small bands near 3080, 2616 and 2460 cm^{-1}. However, during the first gas discharge there were bands at 1376, 1340, 1056 and 896 cm^{-1} that were not present in the second emission. Finally, Fig. 8c also shows the spectrum of a small emission at 528 °C, which is similar to that of the second stage, except for the absence of the bands attributed to methyl and methylenes groups.

3.4.6. Cloisite™ 30B

Fig. 9 shows the obtained results during the thermal degradation of the Cloisite™ 30B, which has two hydroxyl groups in its chemical structure. As expected, the resulting spectra for this sample differ notoriously from those obtained for other organoclays, due to presence of these OH groups. As can be seen in Fig. 9a, the Gram–Schmidt plot showed two main evolved gases zones at 297 and 427 °C. In the first zone, FTIR spectra (see Fig. 9c) showed bands owing of O–H stretching, signals attributed to aliphatic C–H stretching, bands related with CO_2 and a band at 1764 cm^{-1} that might originate from carboxylic acid. Finally, bands related with C–O stretching from alcohol group were also detected. In the second gas discharge, the intensity of the signals attributed to CO_2 and to aliphatic content increased while that related to carbonyl stretching decreased.

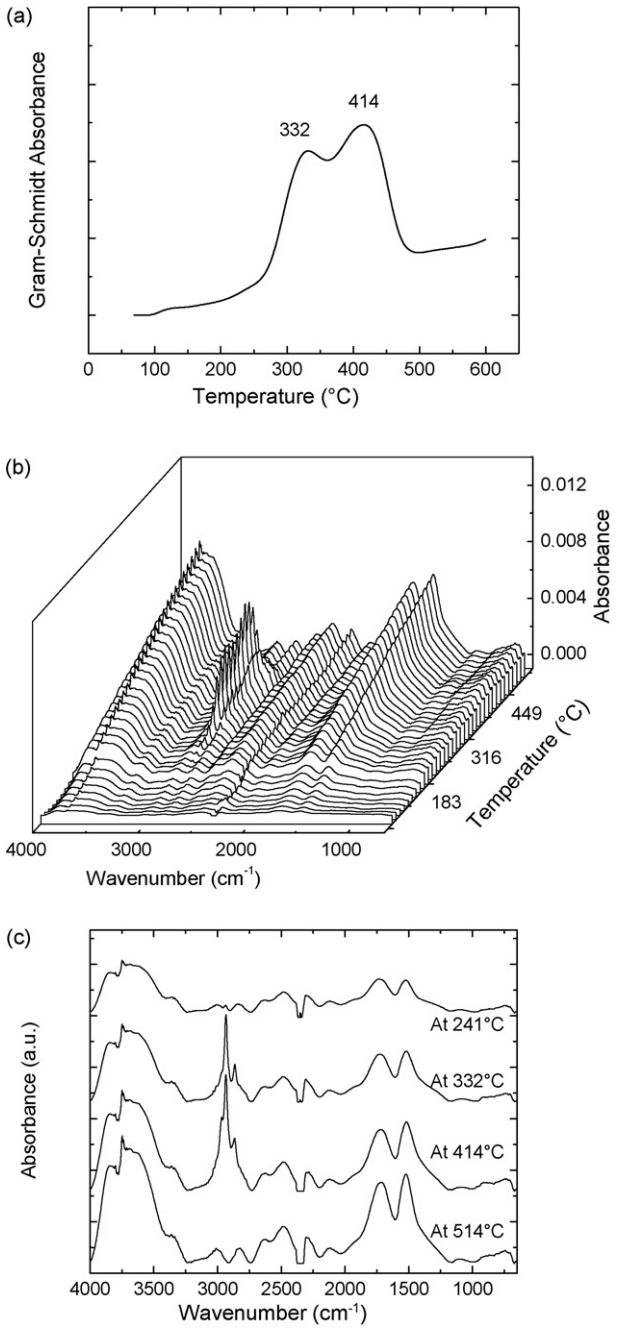

Fig. 7. Gram–Schmidt plot (a); 3D-FTIR spectra of evolved gases (b); and IR spectra obtained at several temperatures (c) for Cloisite™ 20A.

It is worthy of notice that the spectra obtained at 413 and 500 °C (see Fig. 9c) exhibited interesting results and therefore their spectra are also presented. The spectrum collected at 427 °C shows an increasing in the intensity of the peaks corresponding to methyl and methylene groups, while those related with CO_2 disappeared (this indicates that the emission of this gas has stopped). In contrast, bands at 1460, 1388, 1112 and 956 cm^{-1}, which were not clearly defined in spectra of the above temperatures (297 and 413 °C) appeared in that of 427 °C. Finally, in the spectrum obtained at 500 °C, all the bands have vanished and only small bands were noted at 4000–3500, 3016, 2950 and 1528 cm^{-1}. It should be mentioned that a band at ca. 3020 cm^{-1},

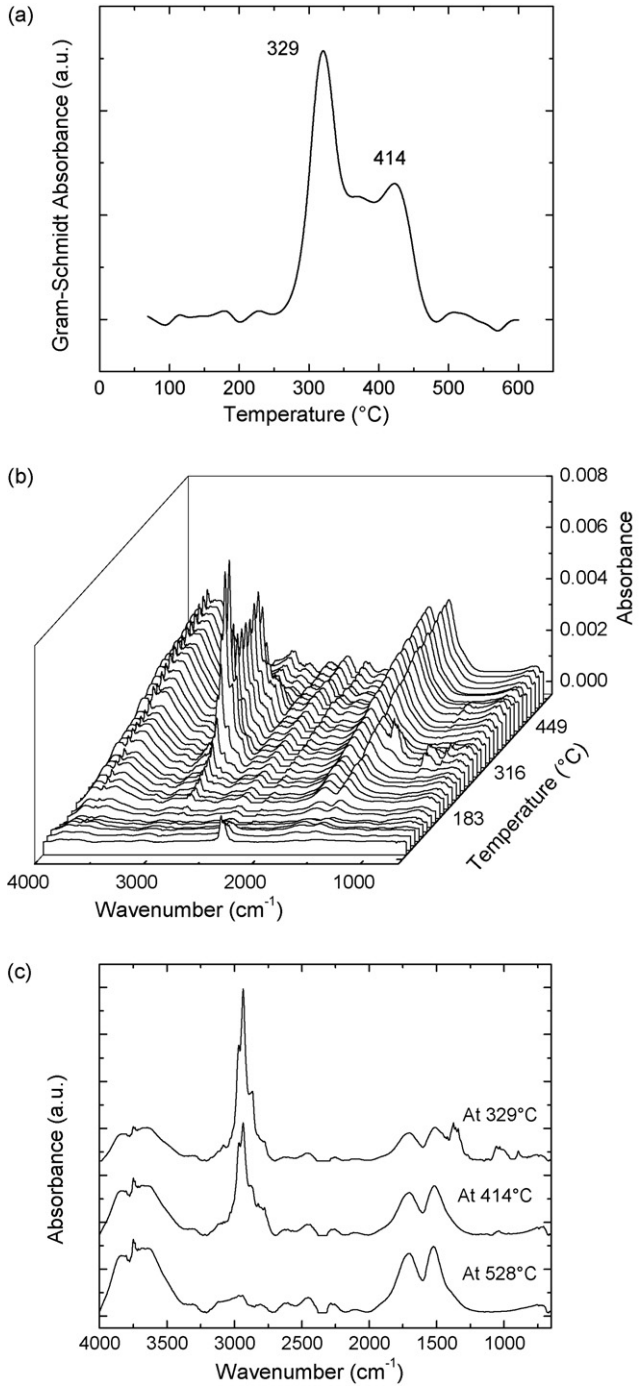

Fig. 8. Gram–Schmidt plot (a); 3D-FTIR spectra of evolved gases (b); and IR spectra obtained at several temperatures (c) for Cloisite^{TM} 25A.

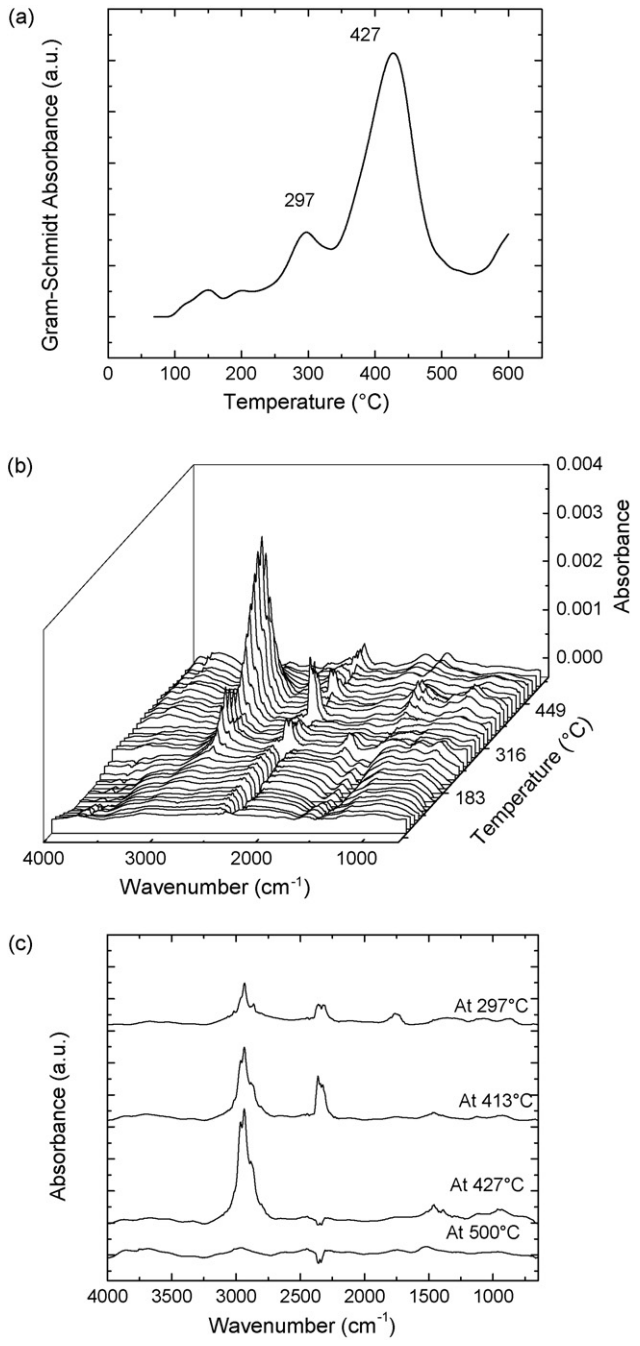

Fig. 9. Gram–Schmidt plot (a); 3D-FTIR spectra of evolved gases (b); and IR spectra obtained at several temperatures (c) for Cloisite^{TM} 30B.

which corresponds to C-H stretching in double bonds, was also observed in all the spectra in Fig. 9c.

3.4.7. Cloisite^{TM} 93A

As noted in Fig. 10, the thermal degradation of this organoclay produces only one evolved gases stage at 409 °C. Correspondingly, FTIR spectrum showed absorption bands attributed to O–H stretching, C–H stretching of methyl and methylene groups and a small band (at 3088 cm^{-1}) related with olefinic compound. Fig. 10c also shows the FTIR spectrum obtained at 528 °C, in which bands attributed to water increased in intensity, while those related to methyl and methylene groups vanished from this spectrum.

4. Discussion

In order to known the chemical reactions that occur during the thermal degradation of alkyl ammonium salts, an analysis of the evolved gases during thermal decomposition was carried out using TGA/FTIR. This technique was chosen because the changes in the chemical composition of the partially degraded

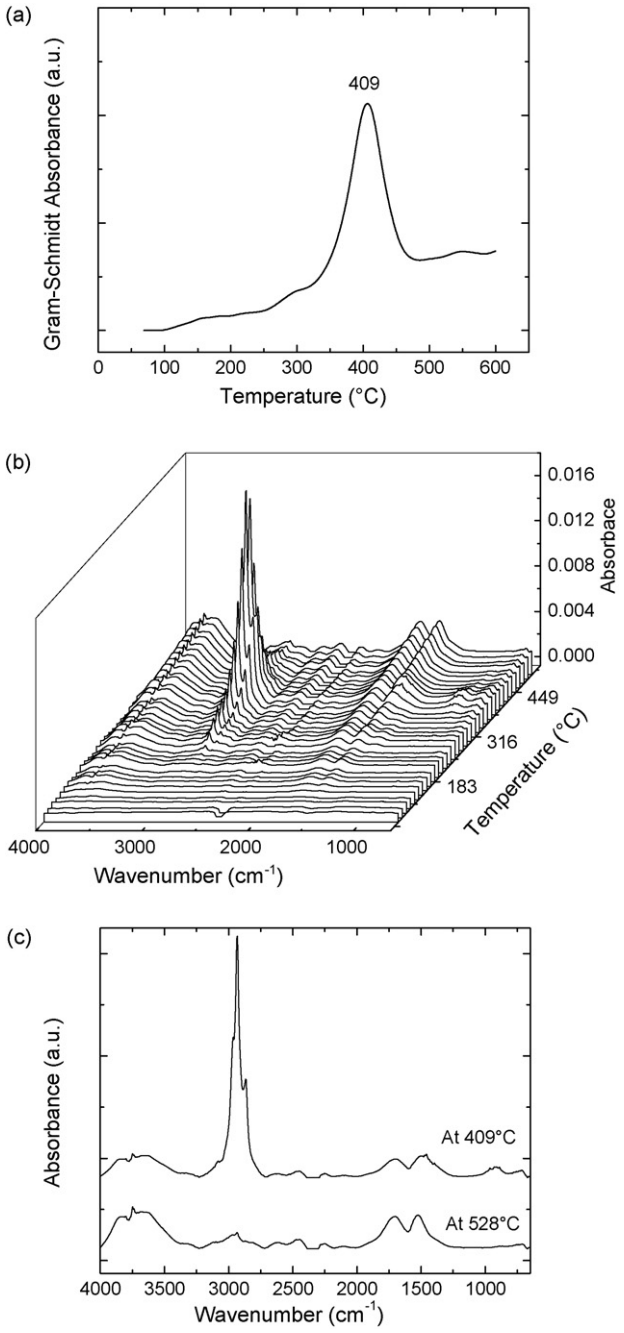

Fig. 10. Gram–Schmidt plot (a); 3D-FTIR spectra of evolved gases (b); and IR spectra obtained at several temperatures (c) for Cloisite^{TM} 93A.

Cloisites^{TM} did not give significant differences in their spectra after degradation of Cloisites^{TM}, except for the disappearance of bands at 2629, 2853 and 1478 cm^{-1}, associated to C–H vibrations of the organic fraction in Cloisites^{TM}. This is due to the small amount of the organic component in the organoclay (ca. 25 wt% for the organic fraction versus ca. 75 wt% for the inorganic part).

It has been proposed that the thermal degradation of organoclays includes desorption of organic ion or/and fragmentation of the organic moiety itself [9]. In the case of Cloisites^{TM}, it follows the typical decomposition reactions of alkyl ammonium salts, which generally proceed either by a Hoffmann elimination reaction or by an SN_2 nucleophilic substitution reactions (see Scheme 1). Hofmann elimination occurs in the presence of a basic anion, such as hydroxide, which extracts a hydrogen atom from the β-carbon of the quaternary ammonium, yielding an olefinic and a tertiary amine group. Nucleophilic attack at elevated temperatures of the chloride onto R_4N^+ favors the reverse of the quaternary ammonium synthesis, yielding RCl and R_3N [6,10]. Taking into account these observations and the chemical composition of the nanoclays, one can suggest *a priori* that Cloisite^{TM} 30B is more prone to Hofmann elimination reaction since its chemical structure has two hydroxyl groups, whereas nucleophilic substitution reaction is more probable for Cloisite^{TM} 15A, since amines, chloroalkanes and alkenes have been found in their degradation products [5]. In addition to the previous mechanism suggested for the thermal degradation of Cloisite^{TM}, we believe that the decomposition of the Tallow (either hydrogenated or dehydrogenated) should also be taken into account. From the organic matter content (ca. 25%wt, see Table 2), the Tallow residue is the main component, whereas nitrogen, associated to the quaternary ammonium salt, account only for the 4%. In more quantitative terms, the molecular weight of Tallow residue could be 5 times higher than a compound containing a nitrogen atom and two methyl groups (M.W. 44 g/mol) commonly present in all types of Cloisites^{TM}. In the following section, the contribution of the tallow fragment to the degradation products will be discussed.

4.1. Analysis of evolved products from TGA–FTIR

In general, Cloisites^{TM} showed IR bands related to water, aliphatic compounds (all except Cloisite^{TM} Na^+) and carbon dioxide (only Cloisite^{TM} 10A and 30B) in 4000–2000 cm^{-1}

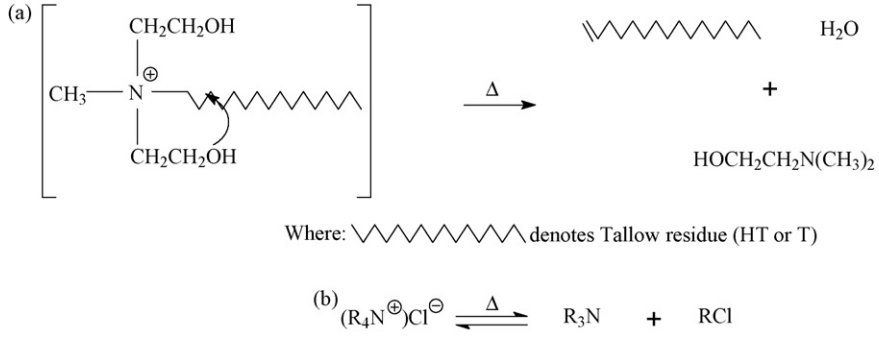

Scheme 1. Schematic representation of (a) Hoffmann elimination reaction; (b) SN_2 nucleophilic substitution reaction.

wavenumber region. Water was identified as a broad band in 4000–3300 cm^{-1} range (O–H stretching) and was corroborated by the presence of bands at 1701 and 1518 cm^{-1} (O–H bending) as can be seen in Figs. 4–10. The previous bands assignment must be taken with caution since many other chemical compounds like alcohols and carboxylic acids also absorbs in this region. For example, Edwards et al. [5] detected the presence of alcohols in the evolved products from thermal decomposition of organoclays.

On the other hand, the existence of aliphatic compounds was noted by the presence of the signals in the 2990–2800 cm^{-1} wavenumber range. These bands were assigned to C–H stretching vibration from methyl and methylene groups from the surfactant. Carbon dioxide was identified by the presence of two bands located at 2364 and 2324 cm^{-1} in agreement with previous reports [6,7]. However, Xie et al. [7] reported evidence of carbon dioxide in the spectra of evolved gases even in sodium Cloisite^{TM}, in opposition to what is shown in the FTIR spectra (see Fig. 4) for the same clay. This contrasting result could be explained by considering the very low content of carbon in our sample, ca. 0.7 wt%, as determined by elemental analysis (see Table 2). In the same line of though, Xie et al. [7] reported bands related to carbon dioxide in all their organically modified montmorillonites at all stages of their thermal decomposition from 200 to 1000 °C. The authors suggested that the absorbed organic matter (alkanes, alkenes) was converted by the aluminosilicate to CO_2; indeed, carbon dioxide could be also formed during the high temperature reaction of carbon present in the surfactant with the oxygen from the crystal structure of the montmorillonite. The above results contradict partially those obtained by us, and therefore, other hypotheses should be considered to explain the presence of CO_2 in the evolved gases from thermal degradation of organoclays. In this line of thought, it must be taken into account the oxidation of residual organic compounds and the presence of a small fraction of insoluble metal carbonate impurities [6].

In the 2000–650 cm^{-1} IR spectral region, the majority of the organically modified clays showed two broad absorption bands centered at ca. 1700 and 1500 cm^{-1}. The broadening of these bands was attributed to the existence of several absorption bands from different functional groups (normal FTIR spectrum in gaseous phase exhibited sharp bands because the effects owing to molecular association are minimized). In order to get more information about these overlapped bands, they were deconvolved in four peaks located at 1773, 1701, 1518 and 1434 cm^{-1} by Gaussian curve-fitting (see Fig. 11). The first band at high frequency, 1773 cm^{-1}, can be assigned to carbonyl stretching vibration of carboxylic acids in gaseous phase [11]. The presence of these structures was confirmed by the presence of bands ca. 2650 cm^{-1}.

As mentioned above, bands at 1701 and 1518 cm^{-1} can be mainly, but not exclusively, related to O–H bending vibration of compounds like water, alcohols, etc., as proposed by Tonsuaadu et al. [12]. Despite this, it is also possible that the band at 1701 cm^{-1} arises from absorptions of aldehyde groups. This was further corroborated by the presence of a band ca. 2775 cm^{-1}, for Cloisite^{TM} 10A, 15A, 20A and 25A which is typical for C–H

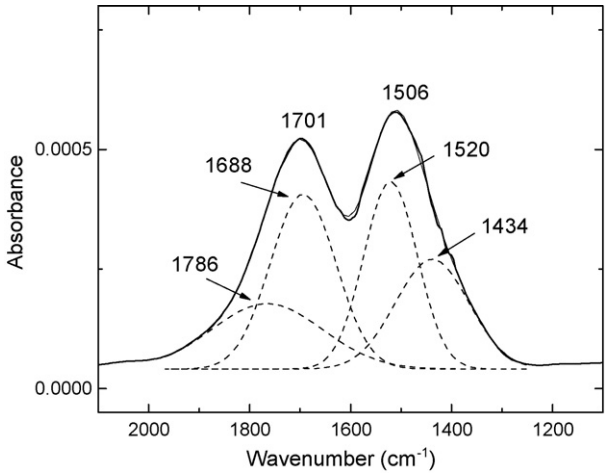

Fig. 11. Deconvolution analysis performed at bands centered at 1700 and 1500 cm^{-1}.

stretching of an aldehyde group. This assignment seems more reasonable, taking into account that Xie et al. [6,7] and Edwards et al. [5] have reported the presence of linear and branched aldehydes in the chemical species evolved from thermal degradation of organically modified clays. In this sense, Edwards et al. [5] reported linear aldehydes, from C7 to C12 and from C16 to C18, for Cloisite^{TM} 30B and 15A, respectively. These results were partially unexpected because the surfactant used for Cloisite^{TM} 15A (see Fig. 1) does not contain oxygen in their structure and the experiments were carried out under non-oxidative conditions. However, it is clear that the aldehydes came from Tallow residue since the molecular weights of aldehydes agree well with the size of these fragments.

In addition to these explanations, we believe that the presence of oxygen (extracted from the crystal structure of the dehydroxylated montmorillonite according to the work of Xie et al. [6]) and alkenes may also yield carboxylic groups which in turn would explain the presence of the band at 1773 cm^{-1} (see Scheme 2). Furthermore, it has been reported that some commercial organoclays made use of non-volatile diluents such as soybean oil for reducing the viscosity of the organoclay formulations [13] or made use of carboxylic acids either as alkyl tail in the quaternary ammonium compound [14] or as the corresponding counter ion [15]. Therefore, the presence of carboxylic groups (and CO_2 after decomposition) may arise from an existing carboxylic acid.

The presence of alkenes, detected at 1518 cm^{-1} and confirmed by the presence of a band at ca. 3020 cm^{-1}, can be explained after Hoffmann elimination reactions [5–7]. However, this hypothesis should be reconsidered as not all the Cloisites^{TM} have hydroxyl moieties in their chemical structure, i.e. they are only present in Cloisite^{TM} 30B. We suggest that the presence of alkenes can also be explained by three possible routes of decomposition: (a) pyrolysis of alkanes derived from the mayor component of the organic part, i.e. hydrogenated tallow; (b) from tallow (unsaturated fatty acids used for the preparation of the quaternary ammonium salt); and (c) decarboxylation of $RCOO^{\bullet}$ and $RCO^{\bullet}$ radicals [10]. The presence of alkenes has been reported by several authors [5–7] in evolved species from Cloisite^{TM} 15A and Cloisite^{TM} 30B.

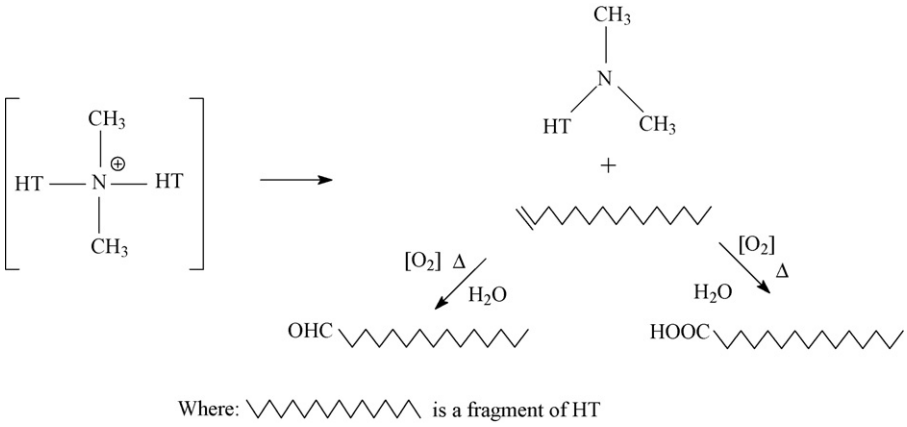

Scheme 2. Suggested reactions to explain the presence of aldehydes and carboxylic acids, in the evolved product from thermal degradation Cloisites™.

Finally, band at 1434 cm^{-1} (obtained from deconvolution analysis) can be attributed to C–H bending from methylene group, confirming the presence of these structures in the evolved gases.

Table 4 summarizes the chemical species evolved for all organoclays samples at several temperatures.

4.2. Influence of surfactant chemical structure on the thermal decomposition of organoclays

The chemical structure of the quaternary alkyl ammonium modifier (surfactant) has a noticeable effect on thermal stability of the organoclay. Thus, replacing a benzyl group (Cloisite™ 10A) by a hydrogenated tallow moiety (Cloisite™ 20A) leads to a more stable organoclay, changing the onset of the decomposition temperature from 160 to 198 °C. Therefore, it is reasonable to assume that the low thermal stability of Cloisite™ 10A is due to the presence of the aromatic structure which was confirmed by the FTIR spectra of the evolved gases at the first stages of its thermal degradation.

Table 4
Chemical species evolved for all organoclays samples at several temperatures

Sample code	Temperature (°C)	Chemical species evolved
Cloisite™ Na^+	300	H_2O
Cloisite™ 10A	126	H_2O, CO_2
	250, 315, 399	H_2O, aromatics, alkanes, alkenes, CHO's, COOH's, amines
	443	H_2O, alkanes, alkenes, CHO's, COOH's
	560	H_2O
Cloisite™ 15A	345, 427	H_2O, alkanes, alkenes, CHO's, COOH's, amines
	570	H_2O, CHO's, COOH's
Cloisite™ 20A	241	H_2O, CHO's, COOH's,
	332, 414	H_2O, alkanes, alkenes, CHO's, COOH's, amines
	514	H_2O, CHO's, COOH's
Cloisite™ 25A	329	H_2O, dialkyl sulfate, alkanes, alkenes, CHO's, COOH's, amines
	414	H_2O, alkanes, alkenes, CHO's, COOH's
	528	H_2O, CHO's, COOH's
Cloisite™ 30B	297	H_2O, CO_2, alkanes, alkenes, CHO's, COOH's, amines
	413	H_2O, CO_2, alkanes, alkenes
	427	H_2O, alkanes, alkenes, alcohols
Cloisite™ 93A	409	H_2O, alkanes, alkenes, CHO's, COOH's, amines
	528	H_2O, CHO's, COOH's

On the other hand, Cloisite™ 93A exhibited a higher decomposition temperature than Cloisite™ 20A. Both clays contain quaternary ammonium cations with two HT substituents and one methyl group being the only difference a methyl group and chlorine anion in Cloisite™ 20A and a hydrogen atom and bisulfate anion in Cloisite™ 93A. One might expect that the thermal stability of Cloisite™ 20A be higher than Cloisite™ 93A as it has been reported that quaternary alkylammonium compounds are more stable than tertiary alkylammonium analogs [16]. Because the opposite behavior was observed in our study, we believe that the thermal stability of quaternary alkylammonium salts depended on the bisulfate anion.

In spite of Cloisite™ 15A and 20A have a similar composition, they exhibited different FTIR spectra during their decomposition. These results may be explained by the fact of that the interlayer distance for Cloisite™ 15A is higher than that reported for 20A (31.5 Å versus 24.2 Å) and by the differences in cation exchange capacity (125 meq/100 g versus 95 meq/100 g). Therefore, desorption of organic compounds will be easier in the clay that has a greater interlayer spacing.

4.3. Specific mechanism of cloisites™ degradation

The presence of bands at 3072, 3036, 1268, 1040, 812 and 700 cm^{-1}, in the evolved products during thermal decomposition of Cloisite™ 10A, may be attributed to the presence of aromatic compounds since the chemical structure of the quaternary alkyl ammonium salt has a benzyl moiety. Therefore, the thermal degradation of this clay could yield aromatic compounds, such as toluene type, and a tertiary aromatic amine, among others compounds.

In the 800–650 cm^{-1} zone, several Cloisites™, whose anion is chloride, presented small signals which are indicative of chlo-

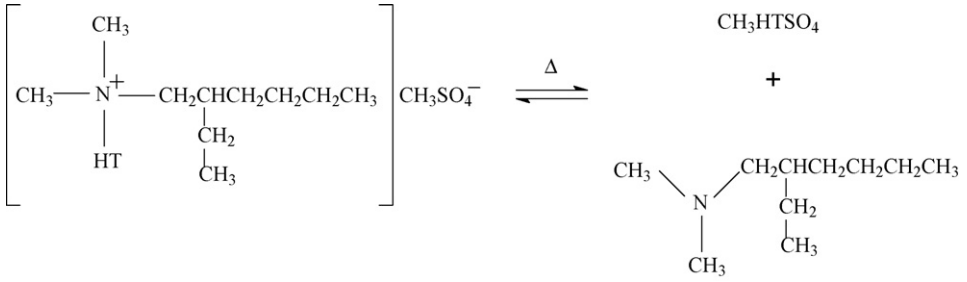

Scheme 3. Schematic representation of SN_2 nucleophilic substitution reaction for the unexchanged surfactant of Cloisite^{TM} 25A.

rinated compounds. For example, Cloisite^{TM} 15A showed a band at 680 cm^{-1}, Cloisite^{TM} 20A exhibited a band at 740 cm^{-1} while Cloisite^{TM} 30B exhibited a band at 750 cm^{-1}. This type of compounds has also been reported by other authors [5–7]. Taking into account these results, it is suggested that this type of compounds came from thermal decomposition of the unexchanged surfactant.

In the case of Closite^{TM} 25A the mechanism that seems to predominate at elevated temperatures in the thermal degradation of this organoclay is the nucleophilic attack, although the attack comes from methyl sulfate ($CH_3SO_4^-$) instead of the chloride anion. Thus, the proposed mechanism will yield a tertiary amine and a dialkyl sulfate (see Scheme 3). This hypothesis was confirmed by the presence of two FTIR bands at 1376 and 1340 cm^{-1}, which were assigned to covalent sulfate absorption (R–O–SO_2–O–R) in a similar manner to that reported by Dyer [17]. The releasing of SO_2 cannot be discarded because this compound possesses bands which absorbs at this wavenumber [12]. Again, following the aforementioned reasoning, we believe that this mechanism is related with unexchanged surfactant. It is important of mention that no other spectrum displayed these signals.

5. Conclusions

In addition to Hoffman elimination reaction and SN2 nucleophilic substitution, an alternative mechanism has been suggested to explain the presence of some degradation products of various types of Cloisites^{TM}. This new mechanism included the thermal degradation of tallow residue and the thermal decomposition of unexchanged surfactant. The former was based on the large amount of tallow present in the organic fraction of the clay while the second can be attributed to an excess of surfactant. These two components allow the formation of carboxylic acid and then the release of CO_2. The chemical structure of the surfactant also played an important role in their thermal decomposition. In this way, the presence of an aromatic residue in the chemical structure of the organic modifier leads to a less stable organoclay. The interlayer dimensions of Cloisites^{TM} galleries as well as the type of anion existing in the surfactant play a key role on the thermal stability of organoclays. FTIR analysis of the evolved products from their non-oxidative conditions showed the release of water, aldehydes, aliphatic compounds and carboxylic acids and, in some cases, aromatic compounds and CO_2. Other decomposition products such as dialkyl sulfate were related with the type of anion present in the organoclay, i.e. methyl sulfate for Cloisite^{TM} 25A.

Acknowledgements

The authors are grateful to Mr. Karl Kamena and Doug Hunter of Southern Clay Co. for technical assistance. We also want to thank Mrs. R. Vargas-Coronado and Mr. W. Herrera-Kao for their assistance in TGA and FTIR experiments.

References

[1] W.H. Awad, J.W. Gilman, M. Nyden, R.H. Harris Jr., T.E. Sutto, J. Callahan, P.C. Trulove, H.C. DeLong, D.M. Fox, Thermochim. Acta 409 (2004) 3–11.
[2] H.J.M. Hanley, C.D. Muzny, D.L. Ho, C.J. Glinka, E. Manias, Int. J. Thermoplast. 22 (2001) 1435–1448.
[3] T.D. Fornes, P.J. Yoon, D.R. Paul, Polymer 44 (2003) 7545–7556.
[4] M. Bora, J.N. Ganguli, D.K. Dutta, Thermochim. Acta 346 (2000) 169–175.
[5] G. Edwards, P. Halley, G. Kerven, D. Martin, Thermochim. Acta 429 (2005) 13–18.
[6] W. Xie, Z. Gao, W.P. Pan, D. Hunter, A. Singh, R. Vaia, Chem. Mater. 13 (2001) 2979–2990.
[7] W. Xie, Z. Gao, K. Liu, W.P. Pan, R. Vaia, D. Hunter, A. Singh, Thermochim. Acta 367–368 (2001) 339–350.
[8] Y. Kim, J.L. White, J. Appl. Polym. Sci. 96 (2005) 1888–1896.
[9] J.W. Lee, Y.T. Lim, O.O. Park, Polym. Bull. 45 (2000) 191–198.
[10] J.W. Alencar, P.B. Alves, A.A. Craveiro, J. Agric. Food Chem. 31 (1983) 1268–1270.
[11] V.A. Basiuk, J.J. Douda, Anal. Appl. Pyrolysis. 60 (2001) 27–40.
[12] K. Tonsuaadu, J. Pelt, M. Borissova, J. Therm Anal. Cal. 80 (2005) 655–658.
[13] C. Cody, B. Campbell, A.Chiavoni, E. Magauran, US Patent 5,634,969 (June 3, 1997).
[14] C.A. Cody, S.J. Kemnetz, European Patent Application 0312988 (October 18, 1988).
[15] W.S. Mardis, C. Malcolm. UK Patent GB 2107693 (October 19, 1981).
[16] R.T. Morrison, R.N. Boyd, Organic Chemistry, fifth ed., Addison-Wesley, Boston, 1987.
[17] J.R. Dyer, Applications of Absorption Spectroscopy of Organic Compounds, first ed., Prentice Hall, New Jersey, 1965.